DOI 10.1007/s10778-017-0821-7
International Applied Mechanics, Vol. 53, No. 4, July, 2017

AXISYMMETRIC ACOUSTOELECTRIC WAVES IN A HOLLOW CYLINDER MADE OF A CONTINUOUSLY INHOMOGENEOUS PIEZOELECTRIC MATERIAL

A. Ya. Grigorenko[1] and I. A. Loza[2]

The propagation of axisymmetric electroelastic waves in hollow cylinders made of a radially polarized functionally gradient piezoceramic material is studied. The material properties vary across the thickness with a power law. The lateral surfaces of the cylinder are free of loads and covered by thin electrodes to which alternating voltage $\pm V_0 \exp[i(kz-\omega t)]$ is applied. To solve the problem, the efficient numerical-analytical method is proposed. The original partial-variable three-dimensional electroelastic problem is reduced, representing components of an elasticity tensor, components of displacement vector, electric-flux density, and electrostatic potential by running waves in an axial direction, to a boundary-value eigen-value problem for ordinary differential equations. This problem is solved with the stable discrete-orthogonolization method. The results of the numerical analysis for the cylinder made of a functionally gradient material (metal and PZT 4 piezoceramics) are presented.

Keywords: kinematic characteristic, propagating electroelastic waves, hollow cylinder, piezoceramic functionally gradient material

Introduction. A great many studies devoted to studying of a wave pattern in the infinitely long elastic cylinders with a circular cross-section have recently appeared. These studies are covered adequately in reviews [2, 15, a.o.] and monographs [1, 5, etc.]. Coupled fields complicate strongly investigations. Thus it appeared to be possible to solve the problem for a piezoceramic cylinder only in terms of special functions in the case of axial polarization of piezoceramics for longitudinal axisymmetric waves and in the case of circumferential polarization for torsional waves. The allowance for the inhomogeneity of the cylinder material all the more complicates the problem, while precisely inhomogeneous piezoelectric materials (bimorphs) are used in many devices. At present, functionally gradient piezoelectric materials, which combine advantages of the bimorphs and free-interface materials, that have different coefficients of thermal expansion, find ever widening application. The attempt to allow for continually varying properties of a material leads to the situation when the material moduli are not constants but functions with respect to one coordinate [8, 9, 13, etc.].This hinders application of many numerical methods.

In what follows, we will consider an axisymmetric problem on propagation of forced acoustoelectric waves in a hollow cylinder with nonuniform thickness made of functionally gradient piezoceramics polarized in a radial direction. The first sets of the solutions of partial differential equations (Lame's equations) in cylindrical coordinates were obtained in studies of Pochhammer [14] and Cree [10, 11]. To solve the above problem, we will employ the efficient numerical-analytical method with which we will analyze the kinematics of acoustoelectric waves propagating along the cylinder axis. The influence of inhomogeneity on the kinematic characteristics of propagating waves will be studied as well.

1. Problem Statement. Basic Equations for Hollow Cylinders. The axisymmetric longitudinal equations of wave motion in a cylindrical coordinate system (r, θ, z) are described as follows:

[1]S. P. Timoshenko Institute of Mechanics, National Academy of Sciences of Ukraine, 3 Nesterova St., Kyiv, Ukraine 03057, e-mail: ayagrigorenko@yandex.ru. [2]National Transport University, 1 Omelyznovicha-Pavlenko St., Kyiv, Ukraine 01010; e-mail: dukeigor@ukr.net. Translated from Prikladnaya Mekhanika, Vol. 53, No. 4, pp. 22–31, July–August, 2017. Original article submitted July 1, 2016.

$$\frac{\partial \sigma_{rr}}{\partial r}+\frac{1}{r}(\sigma_{rr}-\sigma_{\theta\theta})+\frac{\partial \sigma_{rz}}{\partial z}+\rho\omega^2 u_r=0,$$

$$\frac{\partial \sigma_{rz}}{\partial r}+\frac{1}{r}\sigma_{rz}+\frac{\partial \sigma_{zz}}{\partial z}+\rho\omega^2 u_z=0. \tag{1}$$

Equations of electrostatics are:

$$\frac{\partial D_r}{\partial r}+\frac{1}{r}D_r+\frac{\partial D_z}{\partial z}=0, \qquad E_r=-\frac{\partial \varphi}{\partial r}, \qquad E_z=-\frac{\partial \varphi}{\partial z}. \tag{2}$$

Kinematic relations are:

$$\varepsilon_{rr}=\frac{\partial u_r}{\partial r}, \qquad \varepsilon_{\theta\theta}=\frac{1}{r}u_r, \qquad \varepsilon_{zz}=\frac{\partial u_z}{\partial u_z}, \qquad \varepsilon_{rz}=\frac{\partial u_z}{\partial r}+\frac{\partial u_r}{\partial z}, \tag{3}$$

where σ_{ij} are the components of the stress tensor, ρ is the density of the material, ω is the circular frequency, u_i are the components of the displacement vector, D_i are the components of the electric-flux density, E_i are the components of the electric field strength, φ is the electrostatic potential, ε_{ij} are the components of the strain tensor.

The constitutive equations for a piezoelectric material polarized in a radial direction are described as

$$\begin{aligned}
\sigma_{rr}&=c_{33}\varepsilon_{rr}+c_{13}\varepsilon_{\theta\theta}+c_{13}\varepsilon_{zz}-e_{33}E_r, \qquad \sigma_{\theta\theta}=c_{13}\varepsilon_{rr}+c_{11}\varepsilon_{\theta\theta}+c_{12}\varepsilon_{zz}-e_{13}E_r,\\
\sigma_{zz}&=c_{13}\varepsilon_{rr}+c_{12}\varepsilon_{\theta\theta}+c_{11}\varepsilon_{zz}-e_{13}E_r, \qquad \sigma_{rz}=2c_{55}\varepsilon_{rz}-e_{15}E_z,\\
D_r&=e_{33}\varepsilon_{rr}+e_{13}\varepsilon_{\theta\theta}+e_{13}\varepsilon_{zz}+\varepsilon_{33}E_r, \qquad D_z=2e_{15}\varepsilon_{rz}+\varepsilon_{33}E_z,
\end{aligned} \tag{4}$$

where c_{ij} are the components of the tensor of the elastic moduli, e_{ij} are the components of the piezomodulus tensor, ε_{ij} are the components of the permittivity tensor. The above components are functions of a radial coordinate.

Consider a material consisting of two components: steel and piezoceramics. The characteristics of the material vary across the thickness as follows:

$$P(r)=(P_m-P_p)V(r)+P_p, \tag{5}$$

where $V(z)$ is the volume fraction of the ceramics, which is described as

$$V(r)=\left(\frac{r-R_0}{2h}+\frac{1}{2}\right)^n. \tag{6}$$

The boundary conditions on the lateral surfaces of the cylinder (for $r=R_0\pm h$) are: the surfaces are free of external forces: $\sigma_{rr}=\sigma_{rz}=0$ and covered with thin electrodes to which harmonic voltage is applied: $\varphi=\pm V_0 e^{i(kz-\omega t)}$ (R_0 is the radius of the mid-surface of the cylinder; h is the half thickness of the cylinder).

The governing vector of mixed type is:

$$R=\{\sigma_{rr},\sigma_{rz},\varphi,u_r,u_z,D_r\}^T. \tag{7}$$

Resolving system (1)–(4) for the vector R and performing some transformations, we obtain:

$$\frac{\partial \sigma_{rr}}{\partial r}=\frac{1}{r}\left(\frac{c_{12}}{c_{11}}-1\right)\sigma_{rr}-\frac{\partial \sigma_{rz}}{\partial z}+\frac{\Delta_5}{rc_{11}}\frac{\partial \varphi}{\partial z}+\left(\frac{\Delta_4}{r^2c_{11}}-\rho\frac{\partial^2}{\partial t^2}\right)u_r+\frac{\Delta_1}{rc_{11}}\frac{\partial u_z}{\partial z},$$

$$\frac{\partial \sigma_{rz}}{\partial r}=-\frac{c_{13}}{c_{11}}\frac{\partial \sigma_{rr}}{\partial z}-\frac{1}{r}\sigma_{rz}+\frac{\Delta_3}{c_{11}}\frac{\partial^2 \varphi}{\partial z^2}-\frac{\Delta_1}{rc_{11}}\frac{\partial u_r}{\partial z}+\left(\frac{\Delta_2}{c_{11}}\frac{\partial^2}{\partial z^2}-\rho\frac{\partial^2}{\partial t^2}\right)u_z,$$

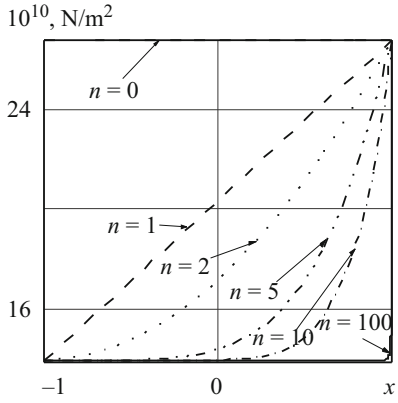

Fig. 1

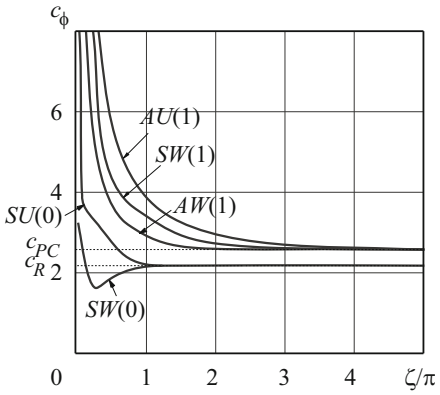

Fig. 2

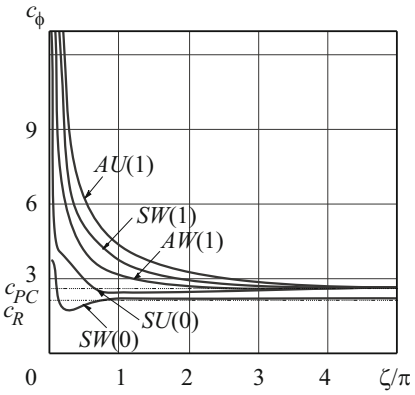

Fig. 3

$$\frac{\partial \varphi}{\partial r} = \frac{e_{15}}{\Delta}\sigma_{rr} - \frac{c_{55}}{\Delta}D_r, \qquad \frac{\partial u_r}{\partial r} = \frac{1}{c_{11}}\sigma_{rr} - \frac{e_{33}}{c_{11}}\frac{\partial \varphi}{\partial z} - \frac{c_{12}}{rc_{11}}u_r - \frac{c_{13}}{c_{11}}\frac{\partial u_z}{\partial z},$$

$$\frac{\partial u_z}{\partial r} = \frac{\varepsilon_{11}}{\Delta}\sigma_{rz} - \frac{\partial u_r}{\partial z} - \frac{e_{51}}{\Delta}D_r, \qquad \frac{\partial D_r}{\partial r} = -\frac{e_{13}}{c_{11}}\frac{\partial \sigma_{rr}}{\partial z} + \frac{\Delta_6}{c_{11}}\frac{\partial^2 \varphi}{\partial z^2} + \frac{\Delta_5}{rc_{11}}\frac{\partial u_r}{\partial z} + \frac{\Delta_3}{c_{11}}\frac{\partial^2 u_z}{\partial z^2} - \frac{1}{r}D_r. \tag{8}$$

2. Method for Solving Axisymmetric Boundary-Value Problems. Let us search for the problem solution in the form of waves running in the axial direction:

$$\sigma_{rr}(r,z,t) = i\lambda\sigma_{rr}(r)e^{i(kz-\omega t)}, \qquad \sigma_{rz}(r,z,t) = \lambda\sigma_{rz}(r)e^{i(kz-\omega t)},$$

$$\varphi(r,z,t) = h\sqrt{\frac{\lambda}{\varepsilon_0}}\varphi(r)e^{i(kz-\omega t)}, \qquad u_r(r,z,t) = ihu_r(r)e^{i(kz-\omega t)},$$

$$u_z(r,z,t) = hu_z(r)e^{i(kz-\omega t)}, \qquad D_r(r,z,t) = \sqrt{\varepsilon_0\lambda}D_r(r)e^{i(kz-\omega t)}. \tag{9}$$

With (9), the original two-dimensional problem of electroelasticity in partial derivatives can be reduced to a boundary-value problem in ordinary differential equations:

$$\frac{dR}{dx} = A(x,\Omega)R \tag{10}$$

with boundary conditions

$$B_1R(-1) = C_1, \qquad B_2R(1) = C_2, \tag{11}$$

where the vector $C_1^T = \{0, 0, -V_0, 0, 0, 0\}$, the vector $C_2^T = \{0, 0, +V_0, 0, 0, 0\}$.

There the following notation is used:

$$\Omega = \omega h\sqrt{\frac{\rho}{\lambda}}, \qquad \tilde{c}_{ij} = \frac{c_{ij}^0}{\lambda}, \qquad \tilde{e}_{ij} = \frac{e_{ij}^0}{\sqrt{\varepsilon_0\lambda}}, \qquad \tilde{\varepsilon}_{ij} = \frac{\varepsilon_{ij}^0}{\varepsilon_0}, \qquad x = \frac{r-R_0}{h},$$

where ρ is the density of the cylinder material, R_0 is the radius of the mid-surface, ε_0 is the vacuum permittivity, $\lambda = 10^{10}$ N/m^2.

The problem is solved by the stable discrete-orthogonalization method.

3. Analysis of Numerical Results. Let us consider results of the numerical analysis of problem (10), (11). Expression (6) is the general formula for the physical-mechanical characteristics of a material, P_p and P_m are the appropriate characteristics

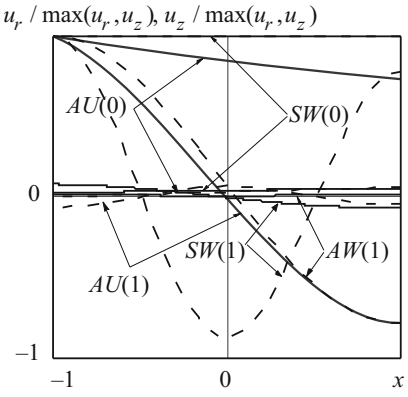

Fig. 4

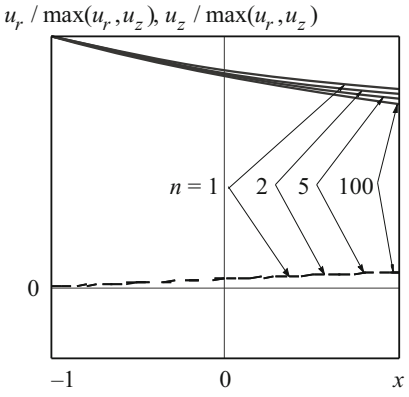

Fig. 5

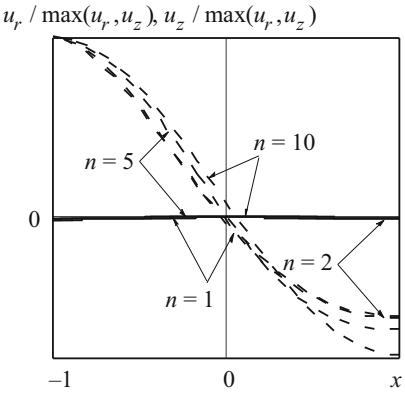

Fig. 6

of the ceramics and metal. The power of the volume fraction of the ceramics in (6) can vary within $0 \le n < 1000$. If $n = 0$, the structure is completely metallic; if $n = \infty$, it is piezoceramic (Fig. 1).

As noted in [11] for a homogeneous problem (free motions), the dispersion relations demonstrate qualitative distinctions. This is better seen from consideration of the phase velocities of propagating waves. Thus the first two waves $SW(0)$ and $AU(0)$ in a short-wave range for a homogeneous cylinder made of PZT 4 piezoceramics (Fig. 2) transform into the Rayleigh-type surface wave. The velocity of these waves is lower than the least from those of body waves in an infinite space:

$$c_R < \min\left(\sqrt{c_{55}/\rho},\ \sqrt{(c_{33} + e_{33}^2/\varepsilon_{33})/\rho}\right).$$

A sophisticated treatment of the displacement distribution in these waves is given below. In the figures, the wave notation is the same as in [7]. The notation $SW(0)$ means that a wave is generated ($k = 0$) as symmetric longitudinal vibrations (planar vibrations), while $AU(0)$ as antisymmetric radial vibrations. The other branches in the short-wave range rather quickly transform into the waves that propagate without dispersion with constant velocity, which exceeds the velocity of the surface waves and is lower than the velocity of the body waves in an infinite space. Let us call these waves as Pochhammer–Cree waves (by analogy with the Lamb waves in a plate).

In the case of an inhomogeneous material, we can see essential transformation in the spectrum of phase velocities. The phase velocities of propagating waves for $n = 5$ are shown in Fig. 3. As is seen, only the first branch transforms into the dispersionless one, while all other propagate with essential dispersion.

If the frequencies are locking ($\zeta = 0$), the purely elastic longitudinal vibrations and coupled electroelastic radial vibrations [7] are held. The analysis of the displacement distributions in running waves in the immediate vicinity of the locking frequencies shows that the motions kept the manner adopted in the notation. Fig. 4 demonstrates how the displacement amplitudes of the first five branches in the homogeneous cylinder ($n = 1000$) ($\zeta = 0.01\pi$) are distributed.

Let us study how the parameter of inhomogeneity affects the distribution of the displacement amplitudes. Thus this influence for the first branch $SW(0)$ is so insignificant that it cannot be presented graphically. The displacements in this wave are mainly longitudinal that is reflected in the notation of this branch. Figure 5 demonstrate how the inhomogeneity parameter influences on the displacement amplitudes for the second branch $AU(0)$ ($\zeta = 0.01\pi$) at different magnitudes of the inhomogeneity factor n. The amplitudes of the radial u_r and longitudinal u_z displacements are shown by solid and dotted lines, respectively. For these waves, the radial displacements dominate. The nearly linear distribution of displacements across the thickness is typical for the branches $SW(0)$ and $AU(0)$. Figures 6–8 show how the inhomogeneity factor n affects the distribution of the displacement amplitudes for the branches $AW(1)$, $SW(1)$, and $AU(1)$, respectively ($\zeta = 0.01\pi$).

If the material is homogeneous, the longitudinal displacements for the $AW(1)$ and $SW(1)$ branches dominate. The number of half-waves per unit increase with the frequency. In the case of an inhomogeneous material, as applied to the $AW(1)$ branch (Fig. 6), the inhomogeneity parameter hardly influences on the manner with which the displacements are distributed. As regards the $SW(1)$ branch (Fig. 7), we should note that variations in the inhomogeneity parameter may result in pronounced changes in the pattern of the displacement distributions. For the high values of the parameter n, i.e. when the cylinder is made, in

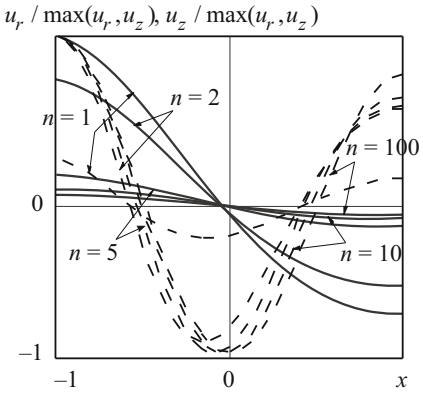

Fig. 7

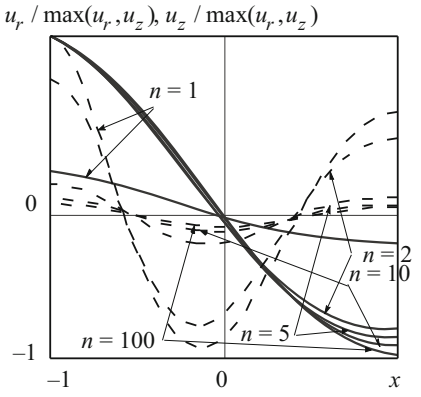

Fig. 8

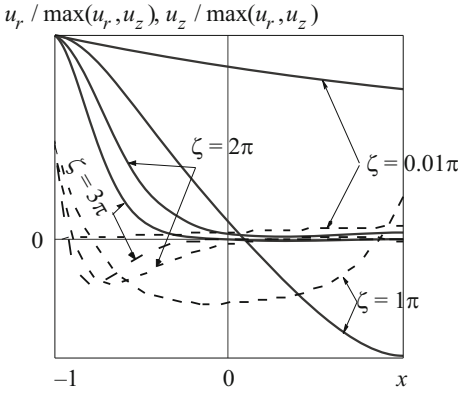

Fig. 9

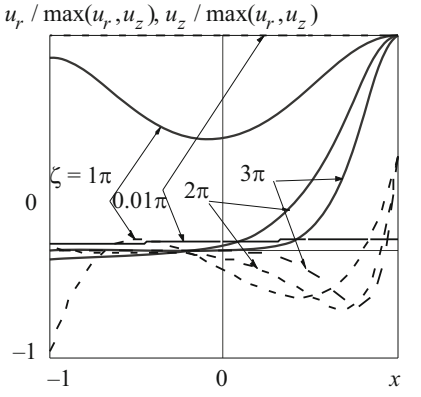

Fig. 10

main, of piezoceramics, the axial displacements dominate (the same way as in the case of a homogeneous piezoceramic material). When the parameter n decreases (the volume fraction of the piezoceramics decreases), the displacements become predominantly radial.

As regards the $AU(1)$ branch (Fig. 8), the radial displacements dominate at high values of the inhomogeneity parameter. This is reflected in the branch notation.

When the parameter of displacement inhomogeneity decreases, the displacements become, in main, longitudinal. The analysis of the plots presented in the above figures demonstrates tendency for the cylinder particles to shift to the lower values of the material moduli.

Consider how the displacement distributions transform across the cylinder thickness with decreasing in the wave length. In the case of a homogeneous material (Fig. 9), the first branch $SW(0)$ approaches the Rayleigh-type surface wave propagating over the inside surface of the cylinder. The second $AU(0)$ branch in the short-wave range approaches the Rayleigh-type surface wave propagating over the inside surface (Fig. 9, heavy line).

In the case of an inhomogeneous material of the cylinder ($n = 5$), we can see qualitative distinctions in the pattern of distribution of the displacement amplitudes. As it was noted above, the first $SW(0)$ branch transforms into the Rayleigh-type surface wave as well (Fig. 11, heavy line). The second $AU(0)$ branch by this time does not transform into Rayleigh-type surface wave (Fig. 12).

In the case of a homogeneous material, the following $AW(1)$ and $SW(1)$ branches (Figs. 13 and 14) in the short-wave range approach to the nearly symmetric (with respect to the cylinder midsurface) or nearly antisymmetric distribution of the displacements across the cylinder thickness. The $AW(1)$ and $SW(1)$ waves ($\zeta = 0$) are generated as longitudinal vibrations, antisymmetric and symmetric, respectively. The displacements become, in main, radial with the decreasing wave length. The radial displacement for the $AW(1)$ wave has one half wave across the thickness, while the longitudinal displacement has two half waves. For the $SW(1)$ wave, the radial displacement has two waves, while the longitudinal displacement has three waves.

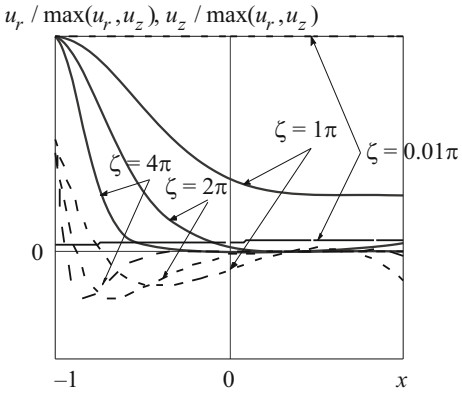

Fig. 11

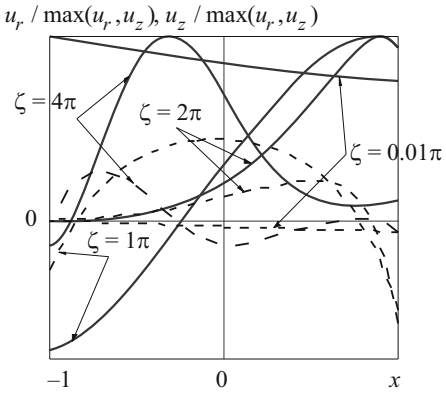

Fig. 12

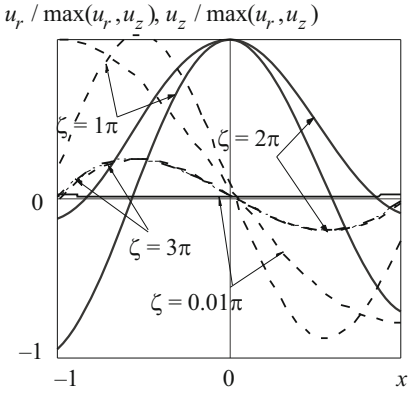

Fig. 13

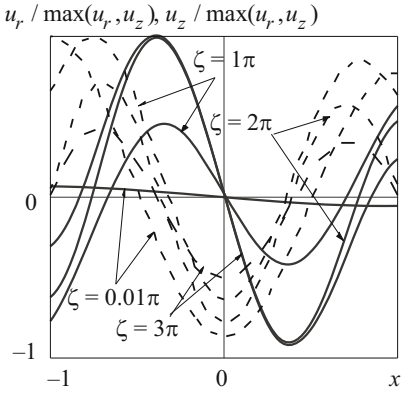

Fig. 14

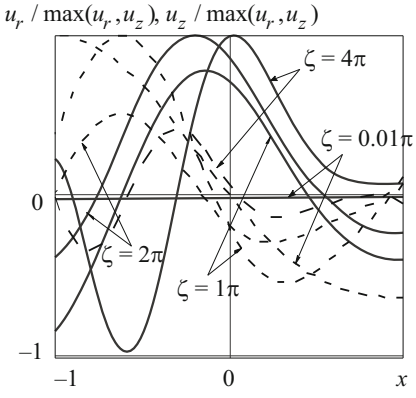

Fig. 15

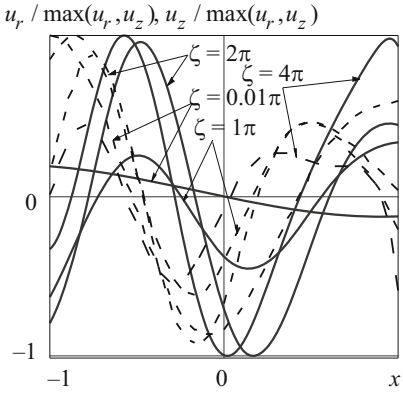

Fig. 16

Such tendency is kept for higher branches: the displacements either nearly symmetric or nearly antisymmetric (with the number of half waves per unit being increased when the serial number of the wave increases by unit).

In the case of an inhomogeneous material, the symmetry of the distribution of displacements about the mid-surface is disturbed. The displacements increase on ”softer” fragments of the cylinder and decrease on more “rigid” ones.

Figure 15 represents the displacement distribution for the $AW(1)$ branch at different values of the wave number. The displacements for the maximum wave number are designated, as above, by heavy lines. The displacement distribution for the $SW(1)$ branch in the case of different wave numbers is shown in Fig. 16.

Conclusions. We have established that the inhomogeneity of the cylinder material causes strong distinctions in the pattern of distribution of the displacement amplitudes of running waves. These distinctions are especially strong in the case of the second branch of the dispersion relations. Thus in the case of a homogeneous material, the first branch in the short-wave range transforms into the Rayleigh-type surface wave propagating over the outside surface of the cylinder. The second branch transforms into the Rayleigh-type surface wave which propagates over the inside surface of the cylinder.

In the case of an inhomogeneous material, only the first branch transforms into the Rayleigh-type surface wave propagating over the surface with minimum moduli values. The second branch does not transform into the surface wave. In the case of the more high branches, the symmetry in the distribution of displacement amplitudes across the thickness and in their shifting to the domain with minimum values of the moduli is broken.

In the case of a homogeneous material, the more high branches in the short-wave range transform into the waves propagating without dispersion. At the same time, the displacement amplitudes are distributed either symmetrically or antisymmetrically with respect to the mid-surface when the number of half waves per unit increases with the wave number. In the case of an inhomogeneous material, the symmetry in distribution of the displacement amplitudes is broken and motions of the cylinder particles shift to the lower values of the moduli.

REFERENCES

1. V. T. Grinchenko and V. V. Meleshko, *Harmonic Vibrations and Waves in Elastic Bodies* [in Russian], Naukova Dumka, Kyiv (1981).
2. G. Kol'skii, *Stress Waves in Solids* [in Russian], Inostr. Lit., Moscow (1955).
3. I. A. Loza, "Propagation of axisymmetric waves in a hollow cylinder made of a functionally gradient piezoelectric material," *Dop. NAN Ukrainy*, No. 3, 50–57 (2015).
4. V. T. Grinchenko, A. F. Ulitko, and N. A. Shul'ga, *Electroelasticity*, Vol. 5 of the five-volume series *Mechanics of Coupled Fields in Structural Members* [in Russian], Naukova Dumka, Kyiv (1989).
5. W. P. Mason and R. N. Thurston (eds.), *Physical Acoustics: Principles and Methods*, Vols. 1–7, Academic Press, New York (1976).
6. N. A. Shul'ga, "Propagation of harmonic waves in anisotropic piezoelectric cylinders: waveguides with complicated properties," Vol. 3 of the six-volume series *Uspekhi Mekh.* [in Russian], A.S.K., Kyiv (2007), pp. 681–702.
7. N. A. Shul'ga, A. Ya. Grigorenko, and I. A. Loza, "Axisymmetric electroelastic waves in a hollow piezoelectric cylinder," *Int. Appl. Mech.*, **20**, No. 1, 23–28, (1984).
8. V. Birman and L. W. Byrd, "Modeling and analysis of functionally graded materials and structures," *ASME Appl. Mech. Rew.*, **195**, 195–216 (2007).
9. Chih-Ping Wu and Tsu-Chieh Tsai, "Exact solutions of a functionally graded piezoelectric material sandwich cylinder by a modified Pagano method," *Appl. Math. Model.*, **36**, No. 5, 1910–1930 (2012).
10. C. Cree, "Longitudinal vibration of a circular bar," *Quart. J. Pure Appl. Math.*, **21**, No. 83/84, 287–298 (1886).
11. C. Cree, "The equations of an isotropic elastic solid in polar and cylindrical coordinates, their solution and application," *Trans. Cambridge Phil. Soc.*, Pt. III, 250–369 (1889).
12. A. Ya. Grigorenko and I. A. Loza, "Axisymmetric waves in layered hollow cylinders with axially polarized piezoelectric layers," *Int. Appl. Mech.*, **47**, No. 6, 707–713 (2011).
13. A. Grigorenko, W. H. Muller, R. Wille, and I. Loza, "Nonaxisymmetric vibrations of radially polarized hollow cylinders made of functionally gradient piezoelectric materials," *Continuum Mech. Thermodyn.*, **24**, No. 4–6, 515–524 (2012).
14. L. Pochhammer, "Uber die fortpfangzungsgeschwindigkeiten kleiner schwingungen in einem unbegrenzten isotropen kreisszylinder," *J. Reine Angew. Math.*, **81**, No. 4, 324–336 (1876).
15. R. N. Thurston, "Elastic waves in rods and clad rods," *J. Accoust. Soc. Am.*, **64**, No. 1, 1–37 (1978).